

# Development of a torsion balance for measuring charging noise

**P Campsie<sup>1</sup>, G D Hammond, J Hough, and S Rowan**

SUPA<sup>2</sup>, Institute for Gravitational Research, School of Physics and Astronomy,  
University of Glasgow, Glasgow, G12 8QQ, UK

E-mail: p.campsie.physics@gmail.com

## **Abstract.**

Noise due to surface charge on gravitational wave detector test masses could potentially become a limiting low frequency noise source in future detectors. It is therefore very important that the behavior of charging noise is experimentally verified so that accurate predictions of charging noise can be made. A torsion balance that is sensitive to small forces has been constructed at the University of Glasgow in order to measure charging noise. In this article the torsion balance apparatus being developed will be described in detail. There will also be a description of the calibration of the instrument and preliminary measurements that have been taken. These measurements show that it is possible to distinguish between the surface charge and polarisation charge on a silica sample. From this measurement it was possible to estimate the surface charge on the silica disc. The remainder of the article will discuss the improvements in sensitivity that have been made which will allow initial measurements of charging noise to begin.

## **1. Introduction**

The detection of gravitational waves still remains one of the most exciting challenges in experimental physics. A worldwide network of six interferometric detectors has been set up to detect gravitational waves generated by astrophysical events. There are three detectors in the US that form the LIGO network [1], one detector located in Italy, Virgo [2], one detector in Germany, GEO600 [3] and one detector in Japan, TAMA 300 [4].

With the beginning of the era of second generation detectors [5, 6, 7] closely approaching, a significant amount of current research in the gravitational wave community is focussed on suppressing the limiting noise sources of these complex instruments in order to maximise the chances of detection. Excess static charges on the detector test masses and suspensions could compromise the sensitivity and control

<sup>1</sup> corresponding author

<sup>2</sup> Scottish Universities Physics Alliance

of the detector and may potentially become a limiting noise source in future detectors [8]. Charging of the test masses can occur through various processes [9]: abrasion with dust as the vacuum chamber is pumped out, contact with nearby structures such as earthquake stops and during cleaning of the test masses with First Contact<sup>TM3</sup>. Another potential source of charging is due to cosmic rays [10, 11, 12] hitting the vacuum chamber walls and showering the test masses in electrons. The excess noise caused by charging is due to charge “hopping”. As electric charge moves around on the dielectric surface of the test mass it creates a fluctuating electric field which gives rise to a fluctuating force which acts on the test mass. It is assumed [13] that these fluctuating forces can be treated as a Markov process with a single correlation time,  $\tau$ , and produce a power spectrum,  $F^2(f)$ , given by:

$$F^2(f) \approx \frac{2\langle F^2 \rangle}{\pi\tau \left( \frac{1}{\tau^2} + (2\pi f)^2 \right)} \quad (1)$$

where  $f$  is frequency and  $\langle F \rangle$  is the average Coulomb force. The displacement noise that arises from surface charging can be expressed as:

$$x(f) = \frac{1}{m(2\pi f)^2} \sqrt{\frac{2\langle F^2 \rangle}{\pi\tau \left( \frac{1}{\tau^2} + (2\pi f)^2 \right)}} \quad (2)$$

where  $m$  is the mass of the optic. This theory has not yet been experimentally confirmed but it is very important that charging noise is measured so that accurate estimates of charging noise in future detectors can be made.

A torsion balance apparatus has been constructed at the University of Glasgow for the purpose of measuring charging noise. A description of the experimental set up, preliminary measurements and investigations into improving the instruments sensitivity will be given in this article. There will also be a brief discussion on the development of a Mark II version of the instrument which should perform even better than the instrument used for the work in this article.

## 2. Experimental setup

### 2.1. The torsion balance apparatus

The torsion balance, shown in Figure 1, consists of a light test mass, hereafter referred to as the bob of the torsion balance, made of aluminium which is suspended by a long thin tungsten fibre which is 50  $\mu\text{m}$  in diameter and 0.6 m in length. The torsion bob consists of a clamping block for the fibre and four arms. There are two copper plates attached to the ends of two opposite arms which are used for position sensing and applying servo control. There are two silica discs on the other arms that are used for charge measurements. A drive signal is applied down the fibre of the torsion balance, using a Stanford SR830 lock in amplifier, in order to provide a signal that can be used for capacitive sensing. This voltage signal has an amplitude of 1 V and a frequency of 100 kHz, which is much greater than the resonant torsional frequency of the bob. The torsion balance has an observed period of 143 seconds ( $\sim 7$  mHz) which compares well

<sup>3</sup> <http://www.photoniccleaning.com/>

to the period calculated from the stiffness of the fibre and the moment of inertia of the bob.

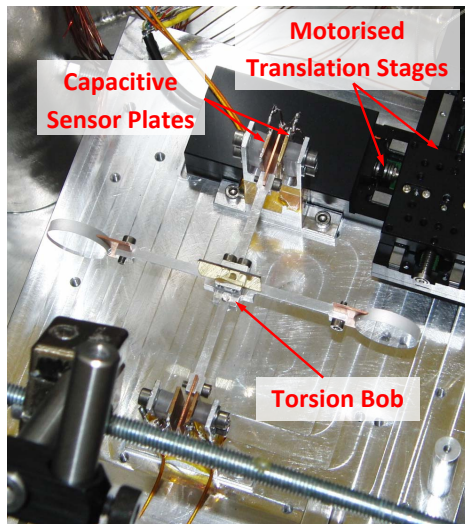


**Figure 1.** A picture of the torsion balance bob.

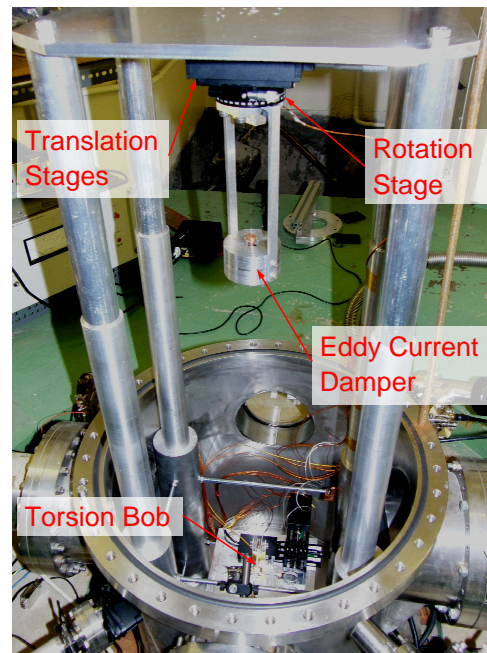


**Figure 2.** A picture of the vacuum tank and inner structure of the tank.

An eddy current damper [14], positioned near the top of the pendulum, is used to damp the pendulum mode of the torsion balance. The eddy current damper is composed of a copper damper disc which has fibre clamps on the top and bottom. The copper disc is enclosed in a housing made of iron which has two neodymium iron rare earth magnets positioned directly above and below the damper disc. As the pendulum mode of the torsion balance is excited, eddy currents are generated in the copper disc which damps the pendulum motion of the bob while the torsional motion of the bob remains unaffected due to the symmetry of the damping disc.

The torsion balance is housed in a vacuum chamber, shown in Figure 2, that can achieve pressures of  $< 1 \times 10^{-5}$  Torr using a BOC Edwards XDS-10 dry scroll pump and a Varian Turbo-V 301 navigator pump. A Varian ConvecTorr gauge was used to monitor the pressure inside the vacuum tank down to  $1 \times 10^{-3}$  Torr and a Varian IMG-100 inverted magnetron gauge was used for pressures below  $1 \times 10^{-3}$  Torr. Inside the vacuum chamber there is an inner structure from which the bob is suspended. The position of the bob can be adjusted using two Thorlabs PT1 translation stages, in an x-y configuration, and a Thorlabs PR01 high precision rotation stage. The rotation stage can be controlled by a stepper motor whilst under vacuum. There is a fixed platform onto which the capacitive sensor plates and two Thorlabs MTS50-Z8E motorised translation stages, in an x-y configuration, are attached (shown in Figure 1). The capacitive sensor is used to monitor the position of the bob and will be discussed in detail later in this

section. The motorised translation stages are used to move charged silica samples near the bob of the torsion balance in order to take a measurement. For the measurements taken in this article a small copper rod was fixed to the motorised translation stages instead of a silica sample. The copper rod was connected to a PC so that sinusoidal voltage signals could be applied to the rod using LabVIEW.

## 2.2. The capacitive sensor

The angular position of the bob is measured using a capacitive sensor. The copper plates that are used for position sensing and applying actuation (located on the bob) sit between two other fixed copper plates, creating what is commonly known as a capacitive bridge. A 1:1:-1 transformer, that consists of two secondary coils and one primary coil, is connected to the pair of capacitive plates that monitor the position of the torsion balance. The positive terminal of the first secondary coil is attached to one sensor plate and the negative terminal of the other secondary coil is attached to the other sensor plate. As mentioned before, the bob of the torsion balance has an AC signal applied to it in order to provide a signal for the sensor. This allows current to flow through the two secondary coils of the transformer and the position of the bob can be deduced from the difference of these currents, the result of which is an induced EMF in the primary coil. The voltage induced in the primary coil is amplified by two low noise inverting op amps (an OPA37 and an AD797) and then the amplified voltage signal is read into a Stanford SR830 lock-in amplifier where it is demodulated into a DC signal. A schematic of the capacitive sensor circuit is shown in Figure 3.

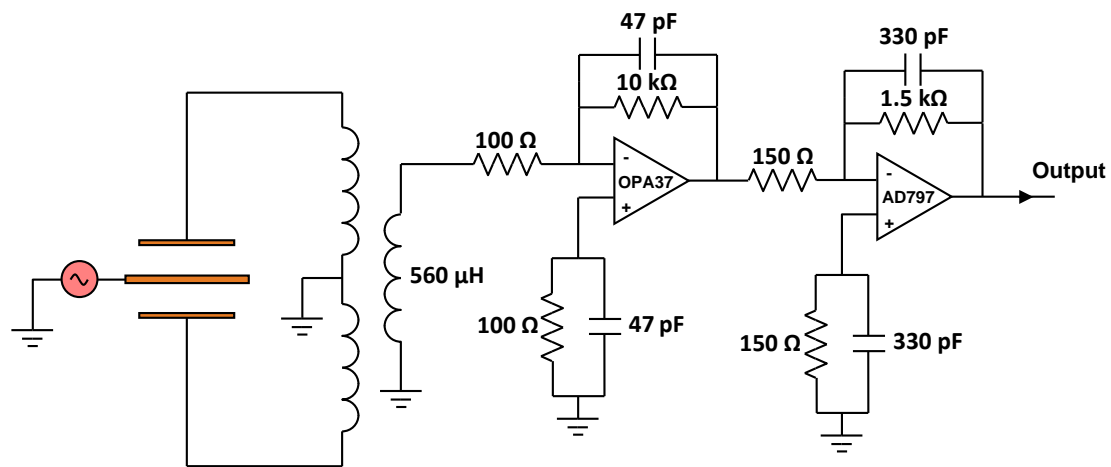


**Figure 3.** A schematic of the capacitive sensor circuit.

The benefit of this capacitive sensor design is that the impedance to ground, through the primary transformer windings, is much less than that due to stray capacitance. Thus all current flows through the windings. The noise of the capacitive sensor, connected to the torsion balance but with no drive signal, at 1 mHz is  $1.62 \times 10^{-4} \text{ V}/\sqrt{\text{Hz}}$  which translates into a torque noise of  $6.02 \times 10^{-14} \text{ Nm}/\sqrt{\text{Hz}}$ .

### 2.3. The PID control

A proportional-integral-derivative (PID) servo control is used to control the position of the torsion balance. In physical terms, proportional control shortens the natural period of the torsion balance, integral control ensures that the torsion balance maintains the set-point and derivative control damps out oscillations of the torsion balance. The voltage signal demodulated by the phase sensitive detector is read onto a PC running a custom PID control program, written in LabVIEW, using a peripheral component interconnect (PCI) 6229 ADC. The program samples a predetermined number of data points from the voltage signal at a selected frequency and performs a linear least squares fit on those data points [15, 16]. The constant parameter of the least squares fit gives the most probable angular position of the torsion balance, which is used in the proportional and integral part of the control program. The gradient of the least squares fit gives the angular velocity of the torsion balance, which is used in the derivative part of the control program. After the program has performed this task it then calculates the output voltages to apply to the servo plates in order to hold the torsion balance in position. The servo control voltage,  $V_{\text{servo}}$ , is given by,

$$V_{\text{servo}} = \alpha (V_{\text{sensor}} - V_{\text{set}}) + \beta \Sigma (V_{\text{sensor}} - V_{\text{set}}) \Delta t + \gamma \frac{dV_{\text{sensor}}}{dt}, \quad (3)$$

where  $\alpha$ ,  $\beta$  and  $\gamma$  are the gains of the P, I and D controls respectively,  $V_{\text{sensor}}$  is the output voltage of the capacitive sensor and  $V_{\text{set}}$  is a programmable set-point.

### 3. Calibration of the torsion balance

In order to calibrate the torsion balance the bob was moved through a known angle and the resulting change in output voltage from the capacitive sensor was measured. It took 49 steps of the stepper motor to move through an angle of  $1^\circ$  and thus 1 step corresponds to an angle of  $356.2 \mu\text{rad}$ . The torsion balance was moved through 2.5 steps and the change in the output voltage of the capacitive sensor was measured. This was repeated for both clockwise and anti-clockwise directions until the bob had been rotated through 5 steps in both directions. A plot of voltage against rotation angle (see Figure 4) was constructed and the gradient of the best fit line through the data gave a value of  $96.1 \mu\text{V}/\mu\text{rad}$ . Once the voltage data had been converted into an angle it was possible to convert it into a torque by dividing it by the response function of the torsion balance,

$$r(f) = \frac{1}{k \left( \left( 1 - \frac{f^2}{f_0^2} \right) + \frac{i}{Q} \right)}, \quad (4)$$

where  $k$  is the stiffness of the fibre,  $f$  is frequency,  $f_0$  is the resonant frequency of the torsion balance and  $Q$  is the quality factor of the torsion balance.

### 4. Initial Results

The torsion balance was set up such that a small copper rod was positioned near one of the silica discs on one arm of the torsion balance. The rod was orientated so that one of its flat circular ends was facing one of the flat circular surfaces of the silica disc. The copper rod had an AC voltage signal of amplitude 1 V and a frequency of 1 MHz applied

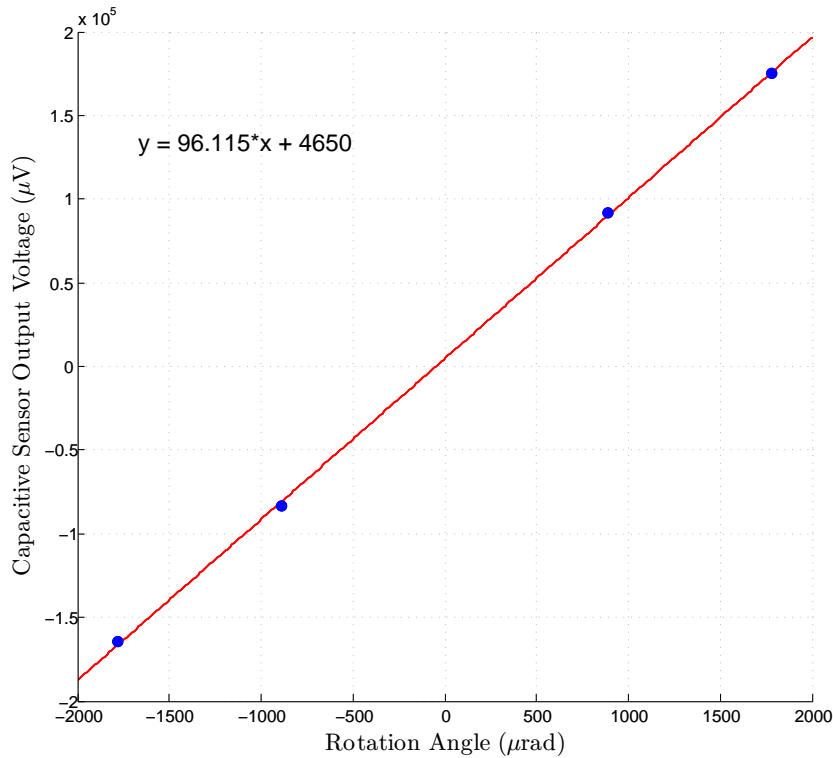


**Figure 4.** A plot of capacitive sensor output voltage against rotation angle. The gradient of the best fit line through the data points was used to calibrate the torsion balance in terms of an angle.

to it. Most of the surface charge was mitigated from the silica disc using a Static Clean International BR2200 rectangular static eliminator bar, however, some residual charge still remained on the disc which interacted with the copper rod. Figure 5 shows an FFT of the time series data from the capacitive sensor. The peaks at 1 mHz and 2 mHz are the  $1\omega$  and  $2\omega$  components of the drive signal respectively, while the signal at 7 mHz is the resonant frequency of the torsion bob. Two peaks arise because the force acting on the torsion balance consists of two contributions. The first is due to the force between the residual surface charge on the silica disc,  $Q_{\text{surface}}$ , and the charge on the copper rod,  $Q_{\text{copper}}$ , and the second is due to the force interaction between  $Q_{\text{copper}}$  and polarisation charges,  $Q_{\text{pol}}$ . Using Gauss's law it is possible to obtain an approximation for  $Q_{\text{copper}}$  that is related to the voltage applied to the rod ( $V$ ),

$$Q_{\text{copper}} = \frac{V\pi r^2 \epsilon_0}{d} \cos \omega t, \quad (5)$$

where  $r$  is the radius of the copper rod,  $d$  is the distance between the surface of the silica disc and the rod,  $\omega$  is the angular frequency of the 1 mHz voltage signal and  $t$  is time. This is then substituted into the equation that describes the force between two charged

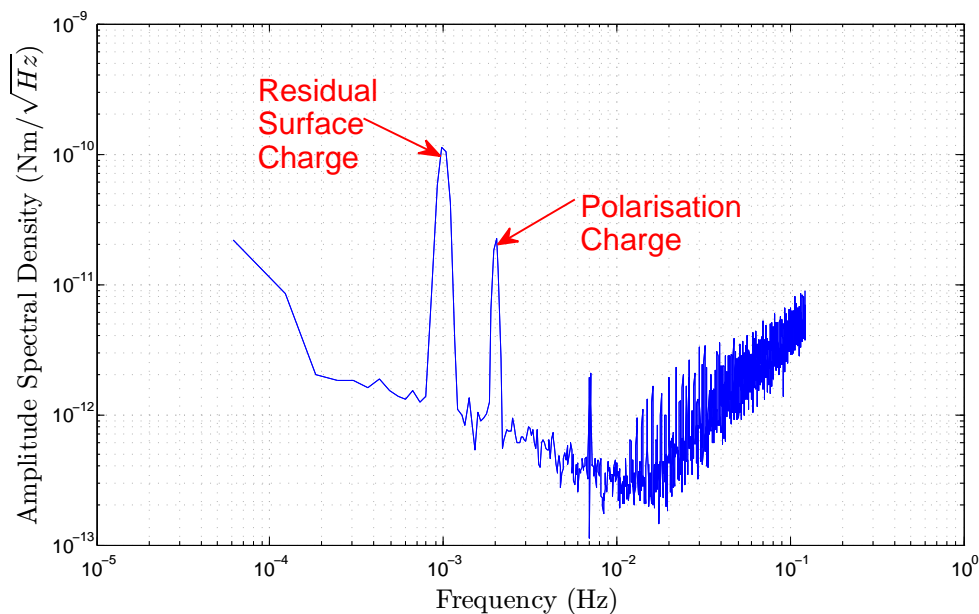


**Figure 5.** Amplitude spectral density of the capacitive sensor output showing a signal due to surface charge interaction at 1 mHz and a signal due to polarisation charge interaction at 2 mHz. The third peak at 7 mHz is the resonant frequency of the torsion bob.

plates to obtain an expression for the force exerted on the torsion balance,

$$F = \frac{(Q_{\text{surface}} + Q_{\text{pol}} \cos \omega t) Q_{\text{copper}}}{2\epsilon_0 \pi r^2}, \quad (6)$$

which becomes,

$$F = \frac{Q_{\text{surface}} V \cos \omega t}{2d} + \frac{Q_{\text{pol}} V \cos^2 \omega t}{2d}. \quad (7)$$

If it is assumed that  $Q_{\text{pol}}$  is small compared to  $Q_{\text{surface}}$  an estimate of the surface charge on the silica disc can be calculated. Using the value for  $F$  calculated from the output voltage of the capacitive sensor a value of  $\sim 2 \times 10^{-14}$  C, which gives an estimated surface charge density of  $1 \times 10^{-9}$  C/m<sup>2</sup>, was obtained. This value agrees well with Kelvin probe measurements, made in a previous publication [17], of residual charge on silica discs after they had been discharged with a corona bar. With the incorporation of a Kelvin probe into this set up it will be possible to calibrate the torsion balance in terms of charge and make surface charge measurements.

## 5. Improving sensitivity

In order to improve the sensitivity of the instrument much effort has gone into identifying and eliminating potential noise sources. One of the first changes that was made was the arrangement of the capacitive sensor plates. Instead of having the sensor plates arranged

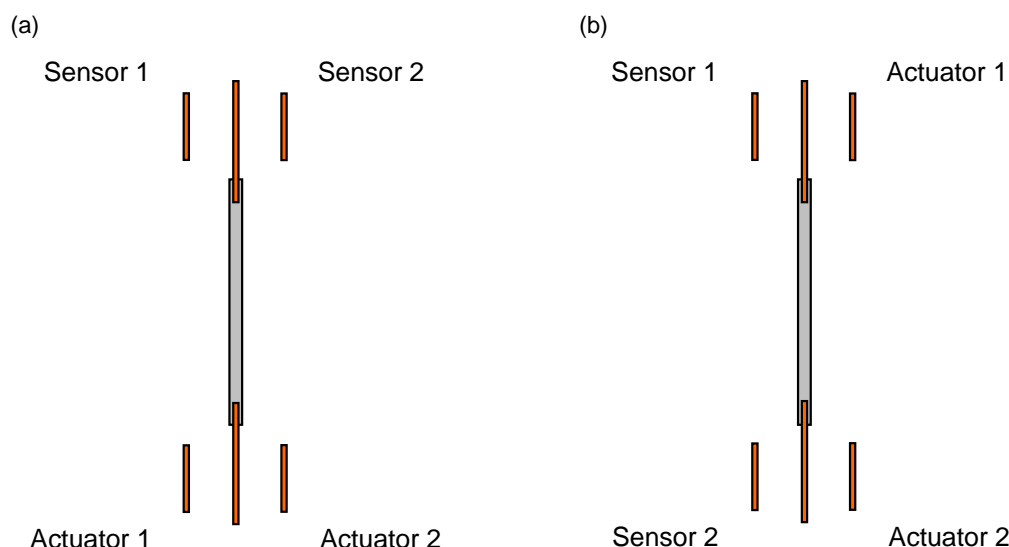


**Figure 6.** A diagram showing (a) the previous arrangement of the position sensor plates and (b) the new arrangement of the position sensor plates.

in the way shown in Figure 6(a) the sensor plates were changed to the set up shown in Figure 6(b). In this configuration the capacitive sensor rejects simple pendulum motion of the bob but remains sensitive to differential rotation of the bob.

A strong correlation was found between the low frequency drift of the torsion balance and temperature drift in the vacuum tank [18]. The temperature is now monitored with three PT-100 thermometers: one outside the vacuum tank, one inside the tank at the top of the tank and another inside the tank at the bottom of the tank. Temperature drift is now removed from the data computationally using a non-linear least squares fit program [19].

A simple copper shield was fabricated that screens the bob from dielectric surfaces. This proved to be very effective in reducing a vast majority of the low frequency noise.

These changes now place the torsion balance at a level of sensitivity capable of measuring charging noise. Figure 7 shows an estimate of the charging noise that would be expected from measurements of touching a silica sample with a copper rod held at a potential of 300 V. The surface charge deposited on the silica sample was  $\sim 1 \times 10^{-11} \text{ C}$  and the correlation time of the charge is assumed to be approximately the same as that measured by Ugolini [9]. Figure 7 also shows the improved torque sensitivity of the torsion balance, the capacitive sensor noise and the thermal noise limit of the instrument. Excess noise is likely due to either seismic noise or dielectric fluctuations due to the fact that there are significant contact potentials present in the apparatus.

## 6. Future work

In order to further improve the sensitivity of the instrument an Applied Geomechanics Inc. 755 miniature tilt sensor was bought to monitor ground tilt. If ground tilt is found



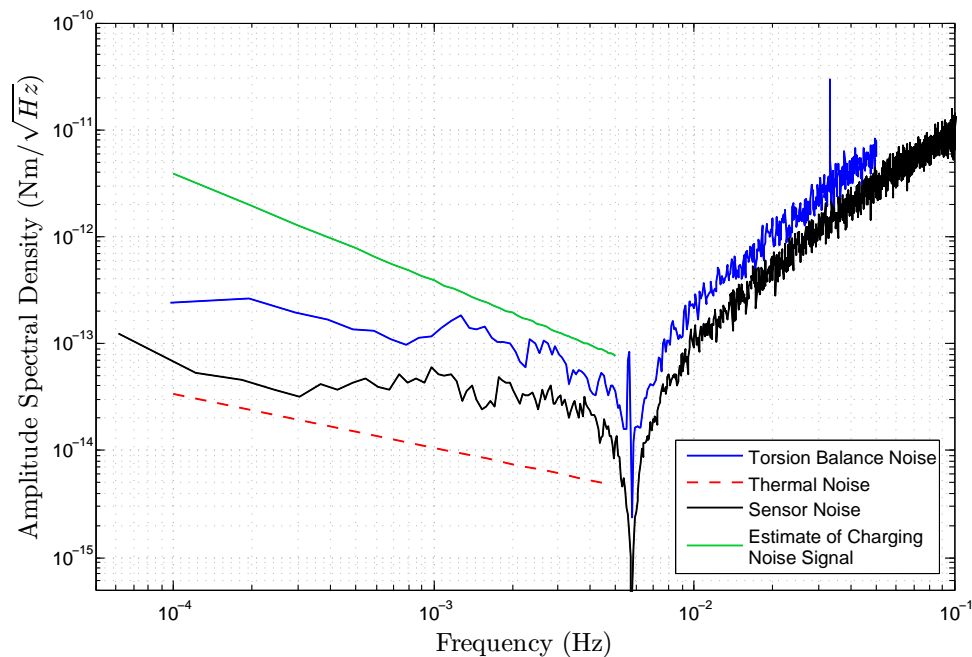


**Figure 7.** The torque noise of the capacitive sensor output (blue). The thermal noise limit (red) sensor noise (black) and an estimate of signal due to charging noise (green) are also featured on the plot.

to be a limiting noise source it will initially be removed computationally in the same manner as the temperature drift but it is planned that eventually a servo controlled tilt table will actively compensate for ground tilt.

It was found that effects of contact potentials [20] arising from the different metals used in the torsion bob are present in the instrument. It is therefore likely that the bob and sensor plates will be coated in gold to eliminate this [21, 22].

The torsion balance bob has been redesigned. The Mark II design will allow the majority of the bob to be grounded while the position is sensed capacitively. There are also plans to incorporate an optical method of monitoring the position of the torsion bob in the Mark II version of the instrument. An optical system should allow the bob to remain completely grounded while still maintaining high sensitivity position sensing.

## 7. Conclusion

A torsion balance has been constructed at the University of Glasgow that will be used to study charging noise. A direct measurement of charging noise has not been made yet and thus a measurement will allow us to confirm whether the Weiss theory of charging noise is the most appropriate description. Initial measurements have shown that it is possible to measure both the polarisation charge and surface charge present on a silica disc. With the inclusion of a Kelvin probe in the experimental set up it should be possible to make accurate measurements of the surface charge on samples of silica. This

will allow accurate estimates of the signal expected from charging noise.

The limiting noise sources of the instrument have been investigated and the sensitivity of the instrument has been greatly improved to the stage where it should be possible to make a successful measurement of charging noise. This measurement will provide greater understanding of charging noise and allow accurate predictions of charging noise in advanced gravitational wave detectors to be made.

### Acknowledgments

We would like to thank the physics department workshop at the University of Glasgow for manufacturing the parts for the work presented in this article and Russell Jones and Michael Perreur-Lloyd (University of Glasgow) for useful discussions on engineering the parts for this work. The authors also gratefully acknowledge the work of Iain McCrindle (University of Glasgow) who built the capacitive sensor circuitry. We are grateful for the financial support provided by Science and Technology Facilities Council (STFC), the Royal Society of Edinburgh (RSE), the Scottish Funding Council (SFC) and the University of Glasgow in the UK. Finally we would like to thank our colleagues in the LSC, the LIGO charging working group and within SUPA for their interest in this work.

### References

- [1] Abbott B P *et al.* 2009 *Rep. Prog. Phys.* **72** 076901
- [2] Accadia T *et al.* 2011 *Class. Quantum Grav.* **28** 114002
- [3] Grote H *et al.* 2010 *Class. Quantum Grav.* **27** 084003
- [4] Takahashi R *et al.* 2004 *Class. Quantum Grav.* **21** S403S408
- [5] Harry G M *et al.* 2010 *Class. Quantum Grav.* **27** 084006
- [6] Acernese F *et al.* 2009 *Advanced Virgo Baseline Design* Internal Virgo Technical Note VIR027A09
- [7] Willke B *et al.* 2006 *Class. Quantum Grav.* **23** S207
- [8] Harry G M 2008 *Estimate of noise from charging in initial, enhanced and advanced LIGO* Internal LIGO Technical Note T080019-01
- [9] Ugolini D, Amin R, Harry G, Hough J, Martin I, Mitrofanov V, Reid S, Rowan S and Sun K X 2008 *International Cosmic Ray Conference* vol 3 pp 1283–1286
- [10] Mitrofanov V P, Prokhorov L G and Tokmakov K V 2002 *Phys. Lett. A* **300** 370–374
- [11] Mitrofanov V P, Prokhorov L G, Tokmakov K V and Willems P 2004 *Class. Quantum Grav.* **21** S1083–S1089
- [12] Braginsky V B, Ryazhskaya O G and Vyatchanin S P 2006 *Phys. Lett. A* **359**(2) 86–89
- [13] Weiss R 1995 *Note on electrostatics in the LIGO suspensions* Internal LIGO Technical Note T960137-00
- [14] Su Y, Heckel B R, Adelberger E G, Gundlach J H, Harris M, Smith G L and Swanson H E 1994 *Phys. Rev. D* **50**(6) 3614–3636
- [15] Savitzky A and Golay M J E 1964 *Anal. Chem.* **36** 1627–1639
- [16] Hammond G D, Speake C C, Matthews A J, Rocco E and Peña-Arellano F 2008 *Rev. Sci. Instrum.* **79**(2) 025103
- [17] Campsie P, Cunningham L, Hendry M, Hough J, Reid S, Rowan S and Hammond G D 2011 *Class. Quantum Grav.* **28** 215010
- [18] Adelberger E G, Stubbs C W, Heckel B R, Su Y, Swanson H E, Smith G, Gundlach J H and Rogers W F 1990 *Phys. Rev. D* **42**(10) 3267–3292
- [19] Linfield G and Penny J 1999 *Numerical Methods using Matlab* 2nd ed (New Jersey: Prentice Hall)
- [20] Pollack S E, Schlamminger S and Gundlach J H 2008 *Phys. Rev. Lett.* **101**(7) 071101
- [21] Schlamminger S, Hagedorn C A and Gundlach J H 2010 *Phys. Rev. D* **81**(12) 123008
- [22] Carbone L, Cavalleri A, Ciani G, Dolesi R, Hueller M, Tombalato D, Vitale S and Weber W J 2006 *AIP Conf. Proc* vol 873 pp 561–565